# Validation of a Clinical PET Scanner Using Monte Carlo Simulation Code: MCNP5

Marianie Musarudin, M.Iqbal Saripan, Syamsiah Mashohor, Wira Hidayat Mohd. Saad
Faculty of Engineering
Universiti Putra Malaysia
Serdang, Malaysia

Suhairul Hashim
Faculty of Science,
Universiti Teknologi Malaysia,
Skudai, Johor, Malaysia

Abdul Jalil Nordin
Center of Diagnostic Nuclear Imaging
Universiti Putra Malaysia
Serdang, Malaysia

***Abstract*— This paper presents a realistic PET scanner simulation using Monte Carlo code, version MCNP5. The objective of our study was to verify the code used for this simulation by comparing the results obtained from the simulation with those obtained from the measurement did on a real PET scanner. This study will provide a basic benchmark for our further study on PET imaging. We modeled the scanner based on the physical specification of Siemens Biograph TruePoint PET scanner. We recorded the generated list-mode data which contains all the information needed to model the PET processes for instance coincidence photon detection. To account for the statistical fluctuations occur in the detector and photomultiplier tube, a Gaussian energy blurring model was applied to the energy deposited in the detector. The scatter and attenuation correction to correct the effect of scattered and attenuated events also took into account in this study. All of these post-simulation processes were done using a program developed using matlab. To validate the simulation, the simulated and measured energy and spatial resolution were compared. We have successfully modeled a PET system based on MCNP5. We also verified that this simulation result in a good agreement data with the real imaging.**

***Keywords- validation; Monte Carlo; PET***

## I. INTRODUCTION

PET image quality is usually influenced by several limitation factors that impede the achievement of a perfect image, for example, physical and biological factors [1]-[7]. The solution for these deficiencies usually studied by researchers with the aid of a tool calls Monte Carlo. The Monte Carlo tool enables of modeling accurate photons interactions for PET system, whereby both photon interactions in the object and in the detector were modeled. There are several specific Monte Carlo codes developed for single photon emission computed tomography (SPECT) and PET, for instance GATE, GEANT4, SimSET, PETSim and GAMOS [3],[8]-[9]. Therefore, previous studies on Monte Carlo modeling of PET system are commonly based on those specific codes [8]-[10]. Therefore, previous reports on validations for PET system modeling are usually reported against those specific codes. This study therefore presents a validation report for PET system modeling against a general Monte Carlo codes, i.e. MCNP5. The purpose of this validation is to provide an accurate model for our further study on PET imaging optimization. Previously, this simulation tool had been used and verified against the real system for single photon emission computed tomography and gamma camera modeling [11]-[15].

There are several methods usually used for validation of nuclear imaging modality simulation [8]-[10]. However, in this study, we focused on two parameters for the simulation code validation. The two parameters are energy and spatial resolution.

In this work, we modeled a realistic PET system using a general Monte Carlo code, version MCNP5. We compared our simulation with the measurement made on Siemens Biograph TruePoint PET in the means of energy resolution and spatial resolution. For validation purposes, the Jaszczak Flangeless Esser PET phantom with a triple line insert which usually used for spatial resolution assessment was used. Recommendations from National Electrical Manufactures Association (NEMA) regarding spatial resolution assessment were followed for this purpose. The contribution of this study is on the development of MCNP5 code for PET scanner simulation and validation of the code against the real PET scanner.

## II. MATERIALS AND METHOD

In this section, the model of the geometry, the algorithm to reconstruct the image and the methods used for the code validation are described in detail.

### A. *MCNP5 simulation of PET scanner*

In this study, the MCNP5 code was done by us. We modeled the complex geometry of PET scanner by definitions of several simple shapes like plane and cylinder in MCNP5 environment. Combination of these simple shapes thus produced the complex geometry desired. The

978-0-7695-5073-2/13 $26.00 © 2013 IEEE
DOI 10.1109/EUROSIM.2013.16

model presented in this paper however is limited to a single ring of detector. The model presented here has been modeled to be realistic as possible with respect to the geometry and physics of photon and charged particle transport. To improve the simulation time, we therefore defined a boundary around the geometry to limit the interaction and thus decreased the simulation time (as showed in fig. 1).

To imitate the geometry of the real scanner, the specifications from Siemens Biograph Truepoint PET were therefore followed (Table 1). The simulated PET scanner was modeled with 48 blocks of scintillation detector arranged in a ring shaped. The detector block was then segmented into 13 smaller detectors with the dimension of 4 x 4 x 20 mm each. The detector was filled with LSO material with density of 7.4 g/cm$^3$. The natural radioactivity of LSO scintillation detector however was not modeled in this study. This is because; the activity of this natural radioactivity is low enough and not significantly influences the clinical setting results [10]. Other than that, the back-compartment structures such as photomultiplier tubes and their assemblies also were not modeled in this study. In this study, the position of the interaction for each photon interaction was calculated based on anger logic, whereby all of the information needed for interaction position determination were provided in the list-mode file recorded from MCNP5 simulation. The position of interaction within the scintillation detector block was calculated as demonstrated by [8]. The equation is:

$$X^j = \frac{\left(\sum_i E_{dep}^i \; X_i^j\right)}{E_{dep}} \tag{1}$$

Whereby $E_{dep}$ is the energy deposited in each detector block and $X_i^j$ is the coordinate of the ith interaction point. Figure 2 shows the example of particles and photons interaction in the model for 10000 particles simulation.

To imitate the real experiment condition, the simulation was performed by setting total number of photon history (nps) based on the following equation [19].

$$nps = A \times 3.7\mathrm{x}10^7 \times t \tag{2}$$

Whereby this equation describing the number of photons emitted by the A mCi radioactivity for t seconds PET imaging protocol.

TABLE 1. SPECIFICATIONS OF SIEMENS BIOGRAPH TRUEPOINT PET SCANNER

| | |
|---|---|
| Detector material | LSO |
| Crystal dimension | 4.0 x 4.0 x 20mm |
| Crystals per detector block | 169 |
| Detector ring diameter | 842 mm |
| Transaxial FOV | 605 mm |
| Axial FOV | 162 mm |

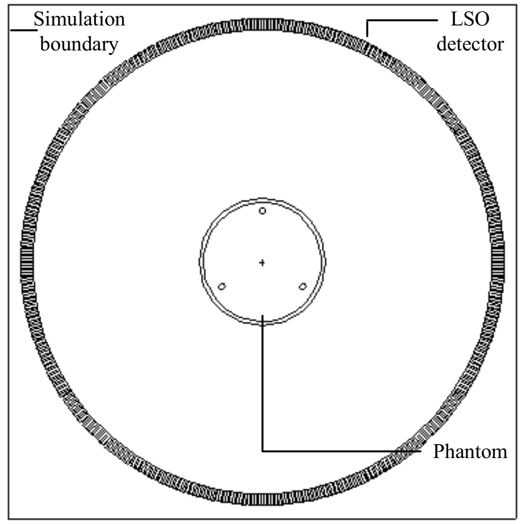


Figure 1. The LSO ring detector and Jaszczak Flangeless Esser PET phantom with a triple line insert at the center of field of view as modeled in MCNP5.

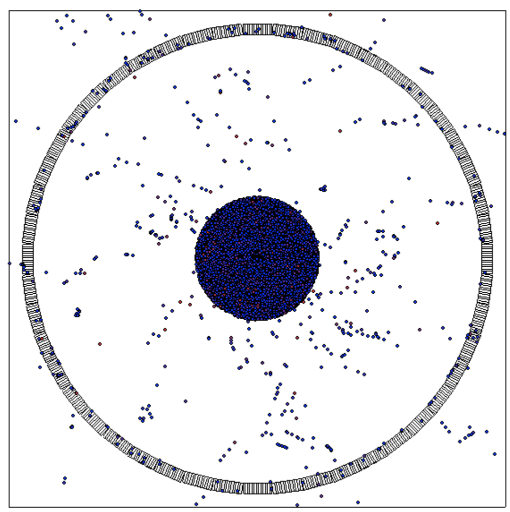

Figure 2. Displays the source and particles/photons interaction as modeled in MCNP5 environment.

## B. *Image reconstruction*

From the simulation, we recorded the PTRAC data which is generally known as list-mode data. The PTRAC file provides all information needed for coincidence photon detection and thus PET image reconstruction, for instance the coordinate of photon interaction, energy and time of interaction. An algorithm to determine the coincidence photons and thus position of interaction was developed by us based on this data. Figure 3 shows the steps of the image reconstruction from the simulation data. To determine the coincidence photons, we first calculated the total energy deposited in the detector block by each photon history as described by Eq. 1. The calculation was done based on our understanding on photons interactions with a medium, as shown in fig. 3. In this study, we put every effort to make the simulated model to be as realistic as possible. Therefore, Gaussian energy blurring was implemented to each of the energy bin to imitate the statistical fluctuation caused by multiple factors in PET imaging. This blurring method was done as demonstrated by [8]. According to them, the Gaussian energy blurring was modeled as following:

$$FWHM = FWHM_{511}\sqrt{511 \times E_{dep}} \quad (3)$$

Whereby $FWHM_{511}$ is the simulated resolution of the system at 511 keV. As recommended by [8], we therefore neglected the small variations of the intrinsic resolution within the detector blocks. The simulated resolution of the system at 511 keV was set to less than 14% as reported in the system specification.

The interactions and thus pair counts were then finally organized into a sinogram. In this study, the sinogram was plotted based on the lines of response which connected the two detector blocks. This study however was limited to a single ring detector, thus restricted the model to one radial directions only for each simulation. To simulate different slices of PET image, we therefore repeat the simulation by changing the position of the detector blocks. To remove the scattered and attenuated photons, the attenuation [16] and scatter correction were performed to the simulated sinogram. In this study, we used filtered back-projection (FBP) algorithm to reconstruct the image.

### C. *Validation of the Model*

The simulated model was validated against the measurement made on Siemens Biograph TruePoint PET. The validation of our simulations was made in two steps. In the first step, we compared the simulated energy resolution with the measured energy resolution. In the second step, the simulated and measured spatial resolution of the corresponding line source was compared. Both parameters were measured by the full width half maximum (FWHM) which is the width of the point spread profile at half of its maximum. This validation process allowed us to validate the accuracy of our simulation code and also the algorithm developed to reconstruct the image.

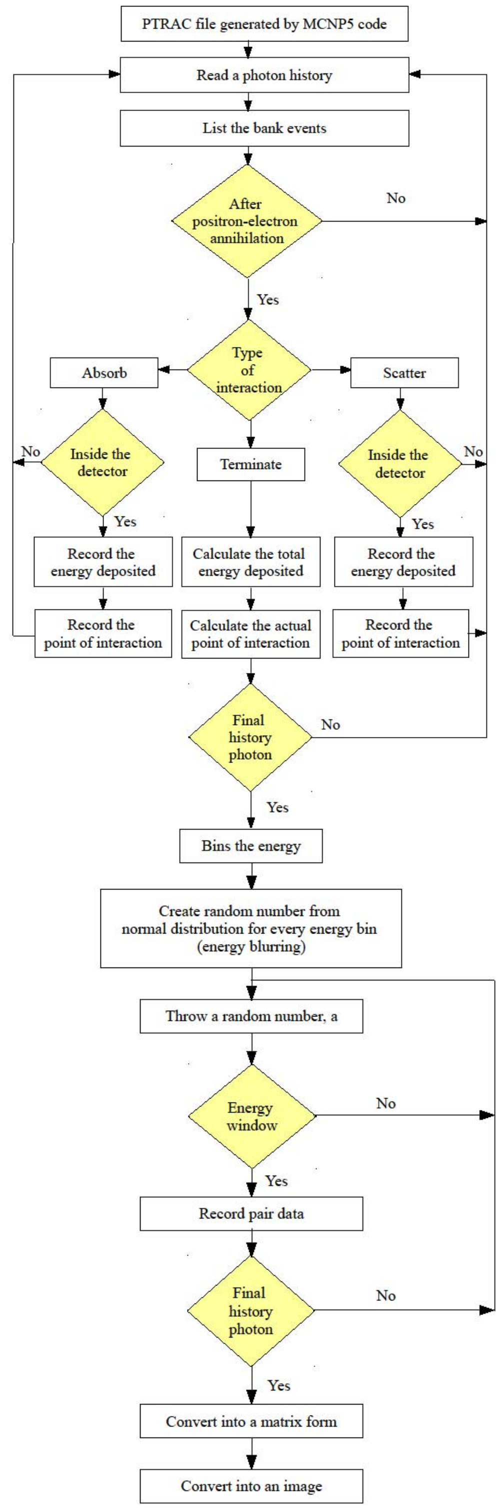


Figure 3. Flow chart of image reconstruction algorithm.

## III. RESULT AND DISCUSSION

### A. Simulated image

Image acquisition was made by using Siemens Biograph TruePoint PET, and the specification of the scanner is listed in Table 1. The measurement was made based on the NEMA recommendation on the spatial resolution. To meet the NEMA recommendation, the random coincidences rate and dead-time losses were ensure to be smaller than 5% of the total event rate. This criterion was achieved by imaging total radioactivity of less than 10 MBq for each acquisition, as demonstrated by [17]-[18].

The line source phantom was positioned at the center of the field of view during the measurement and simulation. Figure 4 and 5 show the sinogram and FBP image reconstructed from the simulation data respectively.

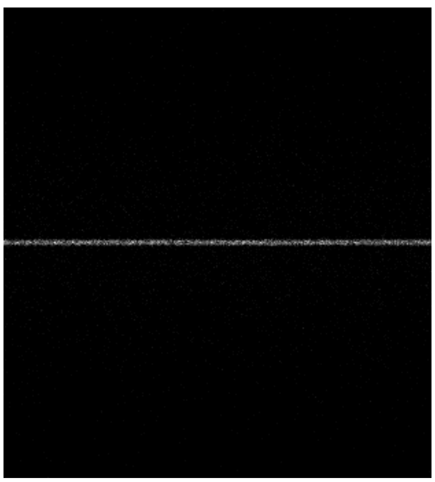

Figure 4. Simulated sinogram using MCNP5 code.

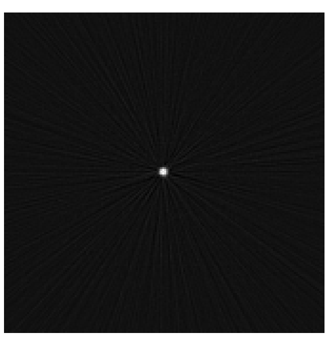

Figure 5. FBP reconstructed image from MCNP5 simulation.

### B. Energy resolution

Figure 6 shows the coincidence energy spectrum obtained from the simulation. Note that, this spectrum shows approximately single peak at 511 keV. This spectrum was plotted before the implementation of the Gaussian energy blurring. To imitate the real imaging condition, we therefore implemented Gaussian energy blurring to the energy bin.

Implementation of Gaussian energy blurring to the energy bins result in a Gaussian shaped spectrum (fig. 7). The energy resolution was measured by measuring the FWHM of the spectrum. This study shows that the implementation of this blurring method produced energy spectrum that is similar to the real imaging condition. Measurement shows that MCNP5 simulation of PET scanner reproduce the energy resolution as specified by the vendor, which is less than 14%.

To improve the efficiency of the program, we therefore implemented the Gaussian energy blurring to the pair coincidence data collected. This was done based on the assumption that each of the pair data energy wills either increases or decreases after the blurring.

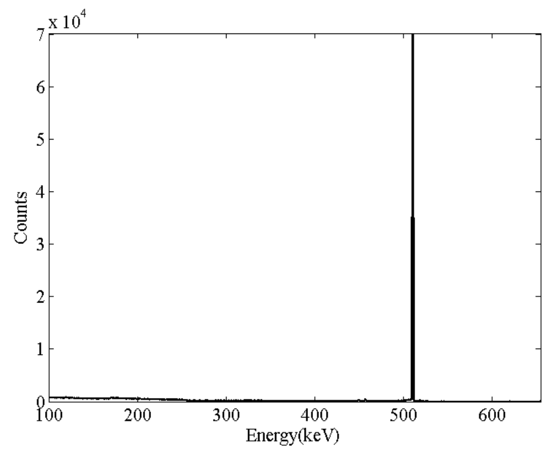


Figure 6. The simulated energy spectrum before Gaussian energy blurring.

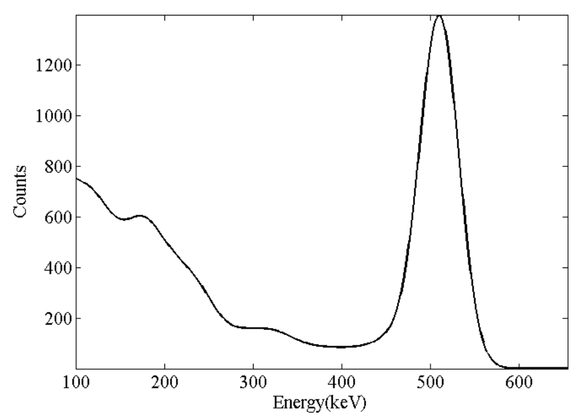


Figure 7. The simulated energy spectrum after Gaussian energy blurring.

### C. *Spatial resolution*

The spatial resolution of the line source was measured and simulated at the center of the field of view, by imaging / simulating the line source filled with Fluorine-18 / positron. The simulated and measured line profiles plotted through the center of the source image are shown in fig. 8 and fig. 9 respectively. For validation purpose, we compare the FWHM of the measured and simulated source image. Results show that the measured and simulated spatial resolution is in good agreement. The measured and simulated spatial resolution was 3.7980 and 3.7909 pixels respectively. The difference between the two was not greater than 0.2%. The good agreement of these results show that the PET image generated by our MCNP5 simulation code fit to the real PET imaging.

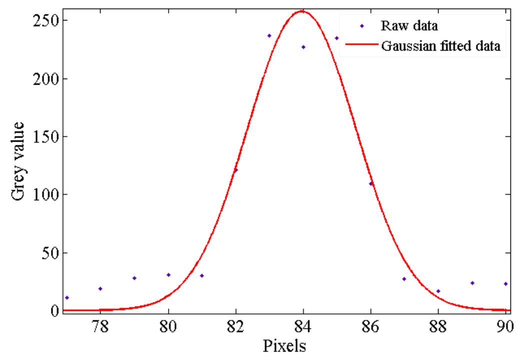


Figure 8. Intensity profile of the simulated image.

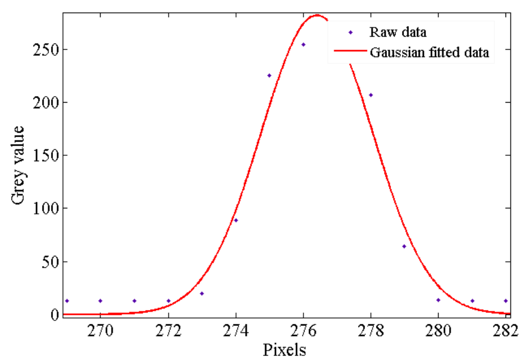


Figure 9. Intensity profile of the scanned image.

## IV. CONCLUSION

We have presented a simple yet realistic Monte Carlo code for PET imaging simulation based on general Monte Carlo version MCNP5. This model had been validated against the experimental results obtained from the real measurement. Comparison shows that the MCNP5 code of PET scanner modeled able to generate the energy resolution of the real PET scanner imaging. In addition, comparison also shows that the spatial resolutions of the simulated and measured images are in a good agreement. Thus, this study proves that our MCNP5 code of PET scanner and also all the post-simulated programs are able to reproduce the condition of the real PET scanner imaging.

## ACKNOWLEDGMENT

This project is partly funded by Sciencefund grant number 06-01-04-SF1183 (5450571) and RUGS grant number 05-03-11-1457RU (9302600).

## REFERENCES

[1] M. R. Ay and S. Sarkar, “Computed tomography based attenuation correction in PET / CT : principles , instrumentation , protocols , artifacts and future trends,” Iran J Nuc Med, vol. 15, pp. 1-29, 2007.

[2] G. Tarantola, F. Zito and P. Gerundini, “PET instrumentation and reconstruction algorithms in whole-body application,” The Journal of Nuclear Medicine, vol. 44, pp. 756-769, 2003.

[3] J. Cal-Gonzalez, J.L. Herraiz, S. Espana, M. Desco, J.J. Vaquero and J.M. Udias, “Positron range effects in high resolution 3D PET imaging,” Nuclear Science Symposium Conference Record (NSS/MIC) IEEE, pp. 2788-2791, 2009.

[4] K. Fiedler, T. Frach, W. Rtten, T. Solf and A. Thon, “Assessment of the spatial resolution of PET scanners using a Geant4-based Monte Carlo tool,” Nuclear Science Symposium Conference Record IEEE, vol. 4, pp. 2549-2553, 2004.

[5] K. Shibuya, E. Yoshida, F. Nishikido, T. Suzuki, T. Tsuda, N. Inadama, T. Yamaya and H. Murayama, “Limit of spatial resolution in FDG-PET due to annihilation photon non-collinearity,” World Congress on Medical Physics and Biomedical Engineering 2006 IFMBE Proceedings, vol. 14, pp. 1667-1671, 2007.

[6] S. Lashkari, S. Sarkar, M. R. Ay, and A. Rahmim, “The influence of crystal material on intercrystal scattering and the parallax effect in PET block detectors: a Monte Carlo study,” IFMBE Proceedings, vol. 21, pp. 633-636, 2008.

[7] P. E. Kinahan, B. H. Hasegawa, and T. Beyer, “X-ray-based attenuation correction for positron emission tomography/computed tomography scanners,” Seminars in Nuclear Medicine, vol. 33, pp. 166-79, Jul. 2003.

[8] B. Guérin and G. El Fakhri, “Realistic PET Monte Carlo Simulation With Pixelated Block Detectors, Light Sharing, Random Coincidences and Dead-Time Modeling,” IEEE Trans Nucl Sci., vol. 55, pp. 942–952, 2008.

[9] L. Le Meunier, F. Mathy, and D. Fagret, “Validation of a PET monte-carlo simulator with random events and dead time modeling,” IEEE Transactions on Nuclear Science, vol. 50, pp. 1462-1468, Oct. 2003.

[10] B. McIntosh, D. B. Stout and A. L. Goertzen, “Validation of a GATE Model of $^{176}$ Lu Intrinsic Radioactivity in LSO PET Systems,” IEEE Transactions on Nuclear Science, vol. 58, NO. 3, JUNE 2011.

[11] M. Alnafea, K. Wells, N.M. Spyrou, M.I. Saripan, M. Guy and P. Hinton, “Preliminary results from a Monte Carlo study of breast tumour imaging with low-energy high-resolution collimator and a modified uniformly-redundant array-coded aperture”, Nuclear Instruments and Methods in Physics Research, Section A: Accelerators, Spectrometers, Detectors and Associated Equipment Vol. 563 (1) , pp. 146-149, 2006.

[12] M.I. Saripan, M. Petrou and K. Wells, “Design of a wire-mesh collimator for gamma cameras”, IEEE Transactions on Biomedical Engineering Vol 54 (9) , pp. 1598-1612, 2007.

[13] M.I. Saripan, W.H. Mohd Saad, S. Hashim, R. Mahmud, A.J. Nordin and M.A. Mahdi, “Monte carlo simulation on breast cancer detection using wire mesh collimator gamma camera”, IEEE Transactions on Nuclear Science Vol 56 (3) , art. no. 5076050 , pp. 1321-1324 , 2009.

[14] W.H.M Saad, R.E. Roslan, M.A. Mahdi, W.S. Choong, E. Saion and M.I. Saripan, "Monte Carlo design of optimal wire mesh collimator for breast tumor imaging process", Nuclear Instruments and Methods in Physics Research, Section A: Accelerators, Spectrometers, Detectors and Associated Equipment, vol. 648 (1), pp. 254-260, 2011.

[15] R.E. Roslan, W.H.M. Saad, M.I. Saripan, S. Hashim and W.S. Choong, "The performance of a wire mesh collimator SPECT camera for different breast volumes in prone position", Nuclear Instruments and Methods in Physics Research, Section A: Accelerators, Spectrometers, Detectors and Associated Equipment, vol. 619 (1-3) , pp. 385-387, 2010.

[16] M. Musarudin, M.I. Saripan, S. Mashohor, W.H.M. Saad, S. Hashim and A. J. Nordin, "Preliminary results from attenuation correction for MCNP-generated PET image," IEEE EMBS International Conference on Biomedical Engineering and Science, pp 907 – 910, 2012.

[17] M. Brambilla, C. Secco, M. Dominietto, R. Matheoud, G. Sacchetti and E. Inglese, "Performance characteristics obtained for a new 3-dimensional lutetium oxyorthosilicate-based whole-body PET/CT scanner with the National Electrical Manufacturers Association NU 2-2001 standard," J Nucl Med., vol. 46, pp 2083-91, 2005.

[18] C.C. Watson, M.E. Casey, L. Eriksson, T. Mulnix, D. Adams and B. Bendriem, "NEMA NU 2 performance tests for scanners with intrinsic radioactivity", J. Nucl. Med., vol. 45, pp. 822– 826, 2004.

[19] B.S. Gopal, "Radioactive decay and interaction of radiation with matter," in Basics of PET imaging: Physics, chemistry and regulations, New York, Springer, 2005, ch. 1, pp. 5-10.

.